IJSES
International Journal of Scientific Engineering and Science
Volume 8, Issue 12, pp. 59-67, 2024.
ISSN (Online): 2456-7361

Finite Element Approximation Based on Mixed Scheme for Fourth Order Equation

Qingqing Yang[1], Jihui Zheng[1,*]
[1]School of Mathematics Science, Guizhou Normal University, Guiyang 550025, China

Abstract— *To establish an efficient finite element approximation for fourth-order equations defined in a circular domain, polar coordinate transformation and orthogonality of Fourier sequence are utilized to decompose the two-dimensional fourth-order problem into a set of independent one-dimensional fourth-order equations, subsequently, an auxiliary second-order equation is introduced to reduce each one-dimensional fourth-order problem to an equivalent second-order mixed formulation. Based on essential pole conditions, a class of weighted Sobolev spaces is defined, and the weak form, as well as its corresponding discrete scheme, is derived for each second-order mixed system. The existence and uniqueness of both the weak and numerical solutions are established using the Lax-Milgram theorem. Additionally, the error estimate between the weak solution and its numerical approximation is obtained using the Céa lemma and the interpolation approximation theorem. Finally, leveraging the properties of piecewise linear interpolation basis functions, the discrete scheme is expressed in its equivalent matrix form, and numerical experiments are presented to validate the algorithm's effectiveness and confirm the accuracy of the theoretical results*.

Keywords— *Fourth-order equation; reduced order scheme; finite element method; error estimation; circular domain*.

I. INTRODUCTION

The fourth-order equation has an important physical background, and in scientific research and engineering calculations, it is often necessary to solve various fourth-order equations [1-3]. The theoretical analysis and numerical solution of fourth-order equations have seen significant advancements. including finite element method[4,7], finite difference method[8,9] and spectrum method[10-12]. However, for the fourth order equations in some special regions (such as circle and sphere), the usual finite element method is not only complicated in region division, but also complicated in basis function construction. Thus, obtaining a highly accurate numerical solution requires considerable computational time and memory resources. Therefore, it is of great significance to propose some high efficiency and high precision numerical methods on special regions.

Therefore, the objective of this paper is to propose an efficient finite element approximation for fourth order equations defined in a circular domain, based on a mixed scheme. First, the original problem is reduced to a series of decoupled one-dimensional second-order hybrid systems. The weak formulation and the corresponding discrete scheme are derived, and the existence and uniqueness of both the weak solution and the numerical solution are established. Additionally, error estimates between the numerical and exact solutions are proved. Second, the discrete scheme is reformulated in matrix form, and several numerical examples are presented to demonstrate the effectiveness of the proposed algorithm and verify the correctness of the theoretical results.

II. DIMENSIONALITY REDUCTION SCHEME AND ITS EQUIVALENT SECOND-ORDER HYBRID SCHEME

This paper considers the following fourth-order equation:

$$\Delta^2 u(x,y)-\alpha\Delta u(x,y)+\beta u(x,y)=f(x,y),\qquad (x,y)\in\Omega, \tag{1}$$

$$u(x,y)=0,\quad \Delta u(x,y)=0,\qquad (x,y)\in\partial\Omega, \tag{2}$$

where: $\Omega=\{(x,y):x^2+y^2\le R^2\}$ is a circle with radius R, $\partial\Omega$ is the boundary of region Ω, α and β are non-negative constants.

By introducing polar coordinates: $x=r\cos\theta, y=r\sin\theta,$ and let $\hat{u}(r,\theta)=u(r\cos\theta,r\sin\theta)$, then the derivative rule of multiple function composition can be obtained:

$$\Delta u(x,y)=\frac{1}{r}\frac{\partial}{\partial r}\left(r\frac{\partial\hat{u}(r,\theta)}{\partial r}\right)+\frac{1}{r^2}\frac{\partial^2\hat{u}(r,\theta)}{\partial\theta^2}. \tag{3}$$

From (3) we can see that equation (1)-(2) has the following equivalent form:

$$\left[\frac{1}{r}\partial_r(r\partial_r)+\frac{1}{r^2}\partial_\theta^2\right]^2\hat{u}-\alpha\left[\frac{1}{r}\partial_r(r\partial_r)+\frac{1}{r^2}\partial_\theta^2\right]\hat{u}+\beta\hat{u}=\hat{f},\qquad (r,\theta)\in D, \tag{4}$$

$$\hat{u}(R,\theta)=0,\ \left[\frac{1}{r}\partial_r(r\partial_r)+\frac{1}{r^2}\partial_\theta^2\right]\hat{u}(R,\theta)=0,\qquad \theta\in[0,2\pi), \tag{5}$$

In formula (4)-(5): $D=(0,R)\times[0,2\pi)$, $\hat{f}(r,\theta)=f(r\cos\theta,r\sin\theta)$. Noting that both $\hat{u}$ and $\hat{f}$ have a period of 2π in the direction of θ, then they can be expanded by Fourier as follows:

$$\hat{u}(r,\theta)=\sum_{|m|}^{\infty}u_m(r)e^{im\theta},\quad \hat{f}(r,\theta)=\sum_{|m|}^{\infty}f_m(r)e^{im\theta}. \tag{6}$$

Substituting (6) into (3) yields:

$$\Delta u(x,y)=\sum_{|m|}^{\infty}[\frac{1}{r}\partial_r(r\partial_r u_m(r))-\frac{m^2}{r^2}u_m(r)]e^{im\theta}. \tag{7}$$

Using the orthogonality of Fourier sequences and (7), equations (4)-(5) can be decomposed into a series of decoupled one-dimensional fourth-order problems as follows:

$$[\frac{1}{r}\partial_r(r\partial_r)-\frac{m^2}{r^2}]^2u_m-\alpha[\frac{1}{r}\partial_r(r\partial_r)-\frac{m^2}{r^2}]u_m+\beta u_m=f_m,\quad r\in(0,R), \tag{8}$$

$$u_m(R)=[\frac{1}{r}\partial_r(r\partial_r)-\frac{m^2}{r^2}]u_m(R)=0. \tag{9}$$

We introduce an auxiliary second order equation:

$$w_m=-[\frac{1}{r}\partial_r(r\partial_r)-\frac{m^2}{r^2}]u_m.$$

then equations (8)-(9) can be reduced to the following equivalent second-order mixed form:

$$-[\frac{1}{r}\partial_r(r\partial_r)-\frac{m^2}{r^2}]w_m+\alpha w_m+\beta u_m=f_m,\quad r\in(0,R), \tag{10}$$

$$-[\frac{1}{r}\partial_r(r\partial_r)-\frac{m^2}{r^2}]u_m-w_m=0,\qquad r\in(0,R), \tag{11}$$

$$m^2u_m(0)=m^2w_m(0)=0, \tag{12}$$

$$u_m(R)=w_m(R)=0. \tag{13}$$

It is important to observe that the boundary condition (12) represents an essential pole condition, which effectively mitigates the singularity arising from the polar coordinate transformation.

III. VARIATIONAL FORM AND DISCRETE FORMAT

In this section, we will establish the variational form of equation (10)-(13) and its discrete scheme. When $\beta=0,$ equations (10)-(13) has been reduced to 2 independent second-order equations. So, it means $\beta>0,$ and let $\omega=r, r\in I=(0,R)$ be a weight function, we make

$$L^2_\omega(I):=\{\rho:\int_I\omega|\rho|^2\,dr<\infty\};$$

$$H^1_{0,\omega,m}(I):=\{\rho:\int_I\omega|\partial_r\rho|^2+m^2\omega^{-1}|\rho|^2\,dr<\infty, m^2\rho(0)=\rho(R)=0\},$$

the corresponding inner product and norm are respectively:

$$(\sigma,\xi)_\omega=\int_I\omega\sigma\xi dr,\qquad \|\sigma\|_\omega=(\int_I\omega|\sigma|^2\,dr)^{\frac{1}{2}};$$

$$(\sigma,\xi)_{1,\omega,m}=\int_I\omega\partial_r\sigma\partial_r\xi+m^2\omega^{-1}\sigma\xi dr,\qquad \|\sigma\|_{1,\omega,m}=(\sigma,\sigma)^{\frac{1}{2}}_{1,\omega,m}.$$

Define the Sobolev space of product type:

$$\mathbf{H}^1_{0,\omega,m}(I):=H^1_{0,\omega,m}(I)\times H^1_{0,\omega,m}(I),$$

the corresponding norm is:

$$\|[\sigma,\xi]\|_{1,\omega,m}=(\|\sigma\|^2_{1,\omega,m}+\|\xi\|^2_{1,\omega,m})^{\frac{1}{2}}.$$

Using the boundary conditions and the integral by parts formula, the variational form of equation (10)-(13) can be obtained as: we find $[w_m,u_m]\in\mathbf{H}^1_{0,\omega,m}(I),$ such that

$$a([w_m,u_m],[v_m,q_m])=f([v_m,q_m]),\quad \forall[v_m,q_m]\in\mathbf{H}^1_{0,\omega,m}(I), \tag{14}$$

where

International Journal of Scientific Engineering and Science
Volume 8, Issue 12, pp. 59-67, 2024. ISSN (Online): 2456-7361

$$a([w_m,u_m],[v_m,q_m])=\int_I r(\partial_r w_m)(\partial_r v_m)+\frac{m^2}{r}w_m v_m+r\alpha w_m v_m+r\beta u_m v_m$$

$$+r\beta(\partial_r u_m)(\partial_r q_m)+\frac{m^2}{r}\beta u_m q_m-r\beta w_m q_m dr,\quad f([v_m,q_m])=\int_I r f_m v_m dr.$$

Using V_h to represent the space formed by the piece-based linear interpolation function, define an approximation space $\mathbf{X}_{mh}(I)=\mathbf{H}^1_{0,\omega,m}(I)\bigcap(V_h\times V_h)$. Then the discrete format of (14) is: Find $[w_{mh},u_{mh}]\in\mathbf{X}_{mh}(I)$, such that

$$a([w_{mh},u_{mh}],[v_{mh},q_{mh}])=f([v_{mh},q_{mh}]),\quad\forall[v_{mh},q_{mh}]\in\mathbf{X}_{mh}(I). \tag{15}$$

IV. THE EXISTENCE AND UNIQUENESS OF THE SOLUTION AND THE ERROR ESTIMATION

In this section, we will establish the existence and uniqueness of both the weak solution and its approximated counterpart, as well as derive an error estimate between them. We represent $a\hat{}\ b$ with the symbol $a\le cb$, where $\boldsymbol{C}$ is a positive constant independent of h.

Lemma 1. The following inequality holds for any $\psi_m\in H^1_{0,\omega,m}(I)$:

$$\int_I r\psi_m^2 dr\hat{}\ \int_I r(\partial_r\psi_m)^2 dr. \tag{16}$$

Proof. From the boundary condition $\psi_m(R)=0$, we get

$$-\psi_m(r)=\int_r^R\partial_r\psi_m(r)dr, \tag{17}$$

It is further obtained by the Cauchy-Schwarz inequality and (17):

$$\int_0^R r\psi_m^2(r)dr=\int_0^R r(\int_r^R\frac{1}{\sqrt{x}}\sqrt{x}\partial_x\psi_m(x)dx)^2dr\le\int_0^R r\int_r^R x(\partial_x\psi_m(x))^2dx(\ln R-\ln r)dr$$

$$\le\int_0^R x(\partial_x\psi_m(x))^2dx\int_0^R r(\ln R-\ln r)dr=\frac{R^2}{4}\int_0^R r(\partial_x\psi_m(x))^2dx=\frac{R^2}{4}\int_0^R r(\partial_r\psi_m(r))^2dr.$$

□

Theorem 1. $a([w_m,u_m],[v_m,q_m])$ is a continuously mandatory bilinear form defined on $\mathbf{H}^1_{0,\omega,m}(I)\times\mathbf{H}^1_{0,\omega,m}(I)$, i.e., for any $([w_m,u_m],[v_m,q_m])\in\mathbf{H}^1_{0,\omega,m}(I)\times\mathbf{H}^1_{0,\omega,m}(I)$ there is

$$|a([w_m,u_m],[v_m,q_m])|\hat{}\ \|[w_m,u_m]\|_{1,\omega,m}\|[v_m,q_m]\|_{1,\omega,m},$$

$$a([w_m,u_m],[w_m,u_m])\%\|[w_m,u_m]\|^2_{1,\omega,m}.$$

Proof. From the Cauchy-Schwarz inequality and (16)

$$|a([w_m,u_m],[v_m,q_m])|\hat{}\ (\int_I r|\partial_r w_m|^2+\frac{m^2}{r}|w_m|^2+r|u_m|^2$$

$$+r|\partial_r u_m|^2+\frac{m^2}{r}|u_m|^2+r|w_m|^2\,dr)^{\frac{1}{2}}(\int_I r|\partial_r v_m|^2+\frac{m^2}{r}|v_m|^2$$

$$+r|v_m|^2+r|\partial_r q_m|^2+\frac{m^2}{r}|q_m|^2+r|q_m|^2\,dr)^{\frac{1}{2}}$$

$$\hat{}\ (\|w_m\|^2_{1,\omega,m}+\|u_m\|^2_{1,\omega,m})^{\frac{1}{2}}(\|v_m\|^2_{1,\omega,m}+\|q_m\|^2_{1,\omega,m})^{\frac{1}{2}}$$

$$\hat{}\ \|[w_m,u_m]\|_{1,\omega,m}\|[v_m,q_m]\|_{1,\omega,m}.$$

On the other hand,

$$a([w_m,u_m],[w_m,u_m])=\int_I r|\partial_r w_m|^2+\frac{m^2}{r}|w_m|^2+r\alpha|w_m|^2+r\beta|\partial_r u_m|^2+\frac{m^2}{r}\beta|u_m|^2\,dr$$

$$\%\int_I r|\partial_r w_m|^2+\frac{m^2}{r}|w_m|^2\,dr+\int_I r|\partial_r u_m|^2+\frac{m^2}{r}|u_m|^2\,dr$$

$$=\|w_m\|^2_{1,\omega,m}+\|u_m\|^2_{1,\omega,m}=\|[w_m,u_m]\|^2_{1,\omega,m}.$$

□

Theorem 2. If $f_m(r)\in L^2_\omega(I)$, then equations (14) and (15) have unique solutions $[w_m,u_m]\in\mathbf{H}^1_{0,\omega,m}(I)$ and $[w_{mh},u_{mh}]\in\mathbf{X}_{mh}(I)$, respectively.

International Journal of Scientific Engineering and Science
Volume 8, Issue 12, pp. 59-67, 2024. ISSN (Online): 2456-7361

Proof. From the Cauchy-Schwarz inequality and Lemma 1:

$$|f([v_m,q_m])|=|\int_I r f_m v_m dr|\le(\int_I r|f_m|^2 dr)^{\frac{1}{2}}(\int_I r|v_m|^2 dr)^{\frac{1}{2}}$$
$$\le\|f_m\|_\omega\|v_m\|_\omega\hat{}\|v_m\|_\omega\hat{}\|\partial_r v_m\|_\omega\hat{}\|v_m\|_{1,\omega,m}$$
$$\hat{}\ (\|v_m\|^2_{1,\omega,m}+\|q_m\|^2_{1,\omega,m})^{\frac{1}{2}}=\|[v_m,q_m]\|_{1,\omega,m}.$$

Then $f([v_m,q_m])$ is a bounded functional on space $\mathbf{H}^1_{0,\omega,m}(I)$. According to theorem 1 and Lax-Milgram theorem, the desired result is valid.

□

Lemma 2. Let $[w_m,u_m]\in\mathbf{H}^1_{0,\omega,m}(I)$ and $[w_{mh},u_{mh}]\in\mathbf{X}_{mh}(I)$ be solutions to equation (14) and (15), respectively, there holds

$$\|[w_m-w_{mh},u_m-u_{mh}]\|_{1,\omega,m}\hat{}\ \inf_{[v_{mh},q_{mh}]\in\mathbf{X}_{mh}(I)}(\|\partial_r(w_m-v_{mh})\|^2+\|\partial_r(u_m-q_{mh})\|^2)^{\frac{1}{2}}.$$

Proof. From (14) and (15) , we have

$$a([w_m-w_{mh},u_m-u_{mh}],[v_{mh},q_{mh}])=0,\forall[v_{mh},q_{mh}]\in\mathbf{X}_{mh}(I).$$

From theorem 1, we have

$$\|[w_m-w_{mh},u_m-u_{mh}]\|^2_{1,\omega,m}\hat{}\ a([w_m-w_{mh},u_m-u_{mh}],[w_m-w_{mh},u_m-u_{mh}])$$
$$=a([w_m-w_{mh},u_m-u_{mh}],[w_m-v_{mh},u_m-q_{mh}])$$
$$=\|[w_m-w_{mh},u_m-u_{mh}]\|_{1,\omega,m}\|[w_m-v_{mh},u_m-q_{mh}]\|_{1,\omega,m},$$

namely

$$\|[w_m-w_{mh},u_m-u_{mh}]\|_{1,\omega,m}\hat{}\ \|[w_m-v_{mh},u_m-q_{mh}]\|_{1,\omega,m}.$$

Next, we will prove the following inequality

$$\|[w_m-v_{mh},u_m-q_{mh}]\|_{1,\omega,m}\hat{}\ (\|\partial_r(w_m-v_{mh})\|^2+\|\partial_r(u_m-q_{mh})\|^2)^{\frac{1}{2}}.$$

When $m=0$, we have

$$\|[w_m-v_{mh},u_m-q_{mh}]\|_{1,\omega,m}=(\int_I r(\partial_r(w_m-v_{mh}))^2dr+\int_I r(\partial_r(u_m-q_{mh}))^2dr)^{\frac{1}{2}}$$
$$\hat{}\ (\int_I(\partial_r(w_m-v_{mh}))^2dr+\int_I(\partial_r(u_m-q_{mh}))^2dr)^{\frac{1}{2}}\hat{}\ (\|\partial_r(w_m-v_{mh})\|^2+\|\partial_r(u_m-q_{mh})\|^2)^{\frac{1}{2}}.$$

When $m\neq0$, It is obtained by polar condition $w_m(0)=u_m(0)=0$ and Hardy inequality

$$\|[w_m-v_{mh},u_m-q_{mh}]\|_{1,\omega,m}$$
$$=(\int_I r(\partial_r(w_m-v_{mh}))^2+\frac{m^2}{r}(w_m-v_{mh})^2+r(\partial_r(u_m-q_{mh}))^2+\frac{m^2}{r}(u_m-q_{mh})^2dr)^{\frac{1}{2}}$$
$$\hat{}\ (\int_I(\partial_r(w_m-v_{mh}))^2+\frac{1}{r^2}(w_m-v_{mh})^2+(\partial_r(u_m-q_{mh}))^2+\frac{1}{r^2}(u_m-q_{mh})^2dr)^{\frac{1}{2}}$$
$$\hat{}\ (\int_I(\partial_r(w_m-v_{mh}))^2+(\partial_r(u_m-q_{mh}))^2dr)^{\frac{1}{2}}=(\|\partial_r(w_m-v_{mh})\|^2+\|\partial_r(u_m-q_{mh})\|^2)^{\frac{1}{2}}.$$

From the arbitrariness of $[v_{mh},q_{mh}]$

$$\|[w_m-w_{mh},u_m-u_{mh}]\|_{1,\omega,m}\hat{}\ \inf_{[v_{mh},q_{mh}]\in\mathbf{X}_{mh}}(\|\partial_r(w_m-v_{mh})\|^2+\|\partial_r(u_m-q_{mh})\|^2)^{\frac{1}{2}}.$$

□

Interval $[0,R]$ is divided as follows:

$$0=r_0<r_1<\cdots<r_{i-1}<r_i<\cdots<r_{N-1}<r_N=R.$$

Let $I_i=[r_{i-1},r_i],h_i=r_i-r_{i-1},h=\max_{1\le i\le N}\{h_i\}$ and define the piecewise linear interpolation operator $I_h=\mathbf{H}^1_{0,\omega,m}(I)\to\mathbf{X}_{mh}(I)$ such that

$$I_h[w_m(r),u_m(r)]=[P_{i1}(r),Q_{i1}(r)],\quad r\in[r_{i-1},r_i],$$

where $P_{i1}(r),Q_{i1}(r)$ represents the linear interpolation function on the interval $[r_{i-1},r_i]$.

International Journal of Scientific Engineering and Science
Volume 8, Issue 12, pp. 59-67, 2024. ISSN (Online): 2456-7361

Lemma 3. If any $r \in I_i$, there is a constant $M > 0$ such that $|\partial_r^2 w_m(r)| + |\partial_r^2 u_m(r)| \le M$, then there holds

$$\| \partial_r (w_m(r) - P_{i1}(r)) \|_{I_i}^2 \hat{} \; h_i^3, \quad \| \partial_r (u_m(r) - Q_{i1}(r)) \|_{I_i}^2 \hat{} \; h_i^3.$$

Proof. It is obtained by linear interpolation

$$P_{i1}(r) = \frac{r - r_i}{r_{i-1} - r_i} w_m(r_{i-1}) + \frac{r - r_{i-1}}{r_i - r_{i-1}} w_m(r_i), \quad r \in I_i.$$

We remember $e_i(r) = w_m(r) - P_{i1}(r), r \in I_i,$, then it holds $e_i(r_{i-1}) = e_i(r_i) = 0.$ And by Rolle's theorem, there exists $\eta_i \in I_i,$ such that

$$\partial_r e_i(\eta_i) = 0.$$

We can notice that

$$|\partial_r e_i(r)| = |\int_{\eta_i}^r \partial_r^2 e_i(r) dr| \,,, (\int_{r_{i-1}}^r 1^2 dr)^{\frac{1}{2}} (\int_{r_{i-1}}^r |\partial_r^2 e_i(r)|^2 \, dr)^{\frac{1}{2}} ,, (r - r_{i-1})^{\frac{1}{2}} (\int_{r_{i-1}}^{r_i} |\partial_r^2 w_m(r)|^2 \, dr)^{\frac{1}{2}}.$$

Thus, we have

$$\| \partial_r (w_m(r) - P_{i1}(r)) \|_{I_i}^2 = \int_{I_i} |\partial_r e_i(r)|^2 \, dr \hat{} \; M h_i \int_{r_{i-1}}^{r_i} (r - r_{i-1}) dr \hat{} \; h_i^3.$$

Similarly, we have

$$\| \partial_r (u_m(r) - Q_{i1}(r)) \|_{I_i}^2 \hat{} \; h_i^3.$$

□

Theorem 3. Let $[w_m, u_m] \in \mathbf{H}_{0,\omega,m}^1(I)$ and $[w_{mh}, u_{mh}] \in \mathbf{X}_{mh}(I)$ be solutions to equations (14) and (15) respectively, then the following estimator holds

$$\| [w_m - w_{mh}, u_m - u_{mh}] \|_{1,\omega,m} \hat{} \; h.$$

Proof. It follows from lemma 2 and Lemma 3,

$$\begin{aligned} \| [w_m - w_{mh}, u_m - u_{mh}] \|_{1,\omega,m}^2 &\hat{} \inf_{[v_{mh}, q_{mh}] \in \mathbf{X}_{mh}} (\| \partial_r (w_m - v_{mh}) \|^2 + \| \partial_r (u_m - q_{mh}) \|^2) \\ &\hat{} \; \| \partial_r (w_m - I_h w_m) \|^2 + \| \partial_r (u_m - I_h u_m) \|^2 \\ &= \sum_{i=1}^N (\| \partial_r (w_m - P_{i1}) \|_{I_i}^2 + \| \partial_r (u_m - Q_{i1}) \|_{I_i}^2) \hat{} \; h^2, \end{aligned}$$

namely

$$\| [w_m - w_{mh}, u_m - u_{mh}] \|_{1,\omega,m} \hat{} \; h.$$

□

V. EFFICIENT IMPLEMENTATION OF THE ALGORITHM

In order to efficiently solve the discrete scheme (15), we need to construct a set of basis functions in the approximation space $\mathbf{X}_{hm}(I)$. We denote by

$$\varphi_0(r) = \begin{cases} \frac{r - r_1}{r_0 - r_1}, & r \in [r_0, r_1], \\ 0, & others, \end{cases} \qquad \varphi_i(r) = \begin{cases} \frac{r - r_{i-1}}{r_i - r_{i-1}}, & r \in [r_{i-1}, r_i], \\ \frac{r - r_{i+1}}{r_i - r_{i+1}}, & r \in [r_i, r_{i+1}], \\ 0, & others, \end{cases}$$

where $i = 1, 2, \cdots, N-1.$ It is clear that

$$\mathbf{X}_{mh}(I) = \text{span}\{\varphi_{sign(|m|)}(r), \cdots, \varphi_{N-1}(r)\} \times \text{span}\{\varphi_{sign(|m|)}(r), \cdots, \varphi_{N-1}(r)\}.$$

We expand the approximate solutions as follows

$$[w_{mh}, u_{mh}] = \sum_{i=sign(|m|)}^{N-1} [w_i^m \varphi_i(r), u_i^m \varphi_i(r)]. \tag{18}$$

Setting

International Journal of Scientific Engineering and Science
Volume 8, Issue 12, pp. 59-67, 2024. ISSN (Online): 2456-7361

$$a_{ni}=\int_I r(\partial_r\varphi_i)(\partial_r\varphi_n)dr,\quad b_{ni}=\int_I r\varphi_i\varphi_n dr,\quad c_{ni}=\int_I \frac{m^2}{r}\varphi_i\varphi_n dr,$$
$$d_{ni}=\int_I \alpha r\varphi_i\varphi_n dr,\quad e_{ni}=\int_I \beta r\varphi_i\varphi_n dr,\quad f_n^m=\int_I r f_m\varphi_n dr.$$

By substituting the formula (18) into the discrete format (15) and letting $[v_{mh}, q_{mh}]$ go through a set of basis functions in $\mathbf{x}_{mh}(I)$, (15) can be reduced to a linear system as follows:

$$\begin{bmatrix}\mathbf{A}_m+\mathbf{C}_m+\mathbf{D}_m & \mathbf{E}_m\\ -\mathbf{B}_m & \mathbf{A}_m+\mathbf{C}_m\end{bmatrix}\begin{bmatrix}\mathbf{W}^m\\ \mathbf{U}^m\end{bmatrix}=\begin{bmatrix}\mathbf{F}^m\\ \mathbf{0}\end{bmatrix},$$

where

$$\mathbf{A}_m=(a_{ni}),\mathbf{B}_m=(b_{ni}),\mathbf{C}_m=(c_{ni}),\mathbf{D}_m=(d_{ni}),\mathbf{E}_m=(e_{ni}),$$
$$\mathbf{W}^m=(w^m_{sign(|m|)},\cdots,w^m_{N-1})^T,\mathbf{U}^m=(u^m_{sign(|m|)},\cdots,u^m_{N-1})^T,\mathbf{F}^m=(f^m_{sign(|m|)},\cdots,f^m_{N-1})^T.$$

VI. NUMERICAL EXPERIMENT

In this section, we will present some numerical examples and program them on the MATLAB R2018b platform. Recalling

$$u(x,y)=\hat{u}(r,\theta)=\sum_{|m|=0}^{\infty}u_m(r)e^{im\theta},$$
$$w=-\Delta u(x,y)=\hat{w}(r,\theta)=\sum_{|m|=0}^{\infty}w_m(r)e^{im\theta}.$$

Let $u_{hM}(x,y), w_{hM}(x,y)$ be the approximate solutions of $u(x,y), w(x,y)$, respectively, i.e.

$$u_{hM}=\sum_{|m|=0}^{M}u_{mh}(r)e^{im\theta},\quad w_{hM}=\sum_{|m|=0}^{M}w_{mh}(r)e^{im\theta}.$$

The error between the exact solution and the approximate solution is defined by

$$e(u,u_{hM})=\|\hat{u}-u_{hM}\|_{L^\infty(D)},\quad e(w,w_{hM})=\|\hat{w}-w_{hM}\|_{L^\infty(D)}.$$

Example 1: We take $\alpha=\beta=1,R=1,u=(x^2+y^2-1)^3e^{\sin(x+y)}$. For different h and M, we list the error between the exact solution and the approximating solution in Tables 1 and 2. In addition, the contrast diagram between the exact solution and the approximating solution is listed in Figure 1 and Figure 2, and the error images between the exact solution and the approximating solution is listed in Figure 3 and Figure 4.

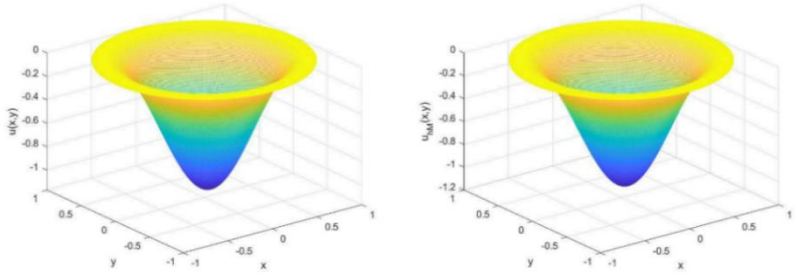

Fig.1 The images of the exact solution u (left) and the approximate solution u_{hM} (right) with $h=1/256, M=12$

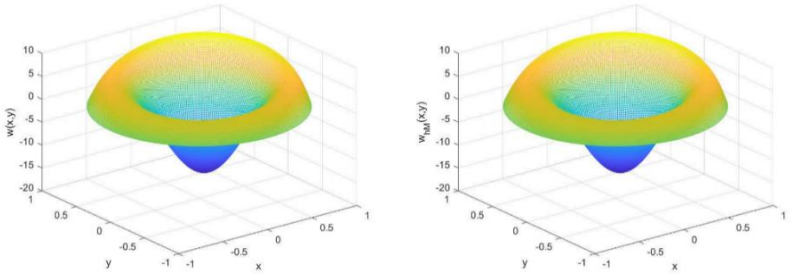

Fig.2 The images of the exact solution w (left) and the approximate solution w_{hM} (right) with $h=1/256, M=12$

International Journal of Scientific Engineering and Science
Volume 8, Issue 12, pp. 59-67, 2024. ISSN (Online): 2456-7361

Tab.1 The error $e(u,u_{hM})$ between the approximate solution u_{hM} and the exact solution u for different h and M

	$M=4$	$M=8$	$M=12$	$M=16$
$h=1/32$	1.6286954×10^{-3}	1.5618842×10^{-3}	1.5619084×10^{-3}	1.5588921×10^{-3}
$h=1/64$	6.0959546×10^{-4}	3.9135296×10^{-4}	3.9137029×10^{-4}	3.9184871×10^{-4}
$h=1/128$	4.3859168×10^{-4}	9.7868639×10^{-5}	9.7889616×10^{-5}	9.7872218×10^{-5}
$h=1/256$	4.2019656×10^{-4}	2.4469335×10^{-5}	2.4488536×10^{-5}	2.4472567×10^{-5}

Tab.2 The error $e(w,w_{hM})$ between the approximate solution w_{hM} and the exact solution w for different h and M

	$M=4$	$M=8$	$M=12$	$M=16$
$h=1/32$	4.9769406×10^{-2}	1.6060392×10^{-2}	1.6372152×10^{-2}	6.3393353×10^{-2}
$h=1/64$	4.2599925×10^{-2}	3.9927816×10^{-3}	4.2889671×10^{-3}	4.0355351×10^{-3}
$h=1/128$	4.1512218×10^{-2}	1.0528577×10^{-3}	1.2635375×10^{-3}	1.0086937×10^{-3}
$h=1/256$	4.1375717×10^{-2}	3.4496374×10^{-4}	5.2965178×10^{-4}	2.8887940×10^{-4}

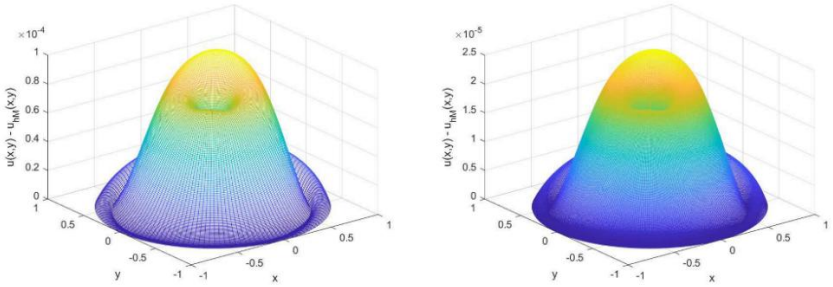

Fig.3 The error images between the exact solution and the approximate solution with $h=1/128, M=8$ (left) and $h=1/256, M=16$ (right)

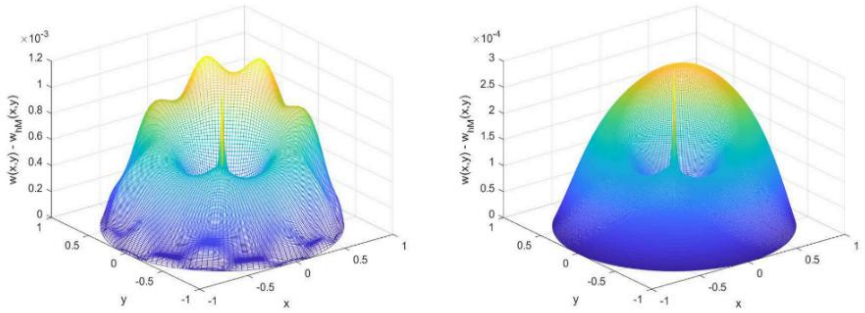

Fig.4 The error images between the exact solution and the approximate solution with $h=1/128, M=8$ (left) and $h=1/256, M=16$ (right)

As can be seen from Table 1-2, the error between the approximate solution and the exact solution decreases with the increase of $1/h$ and M .At $h\le1/128, M\ge8$, approximating solution $u_{hM}(x,y)$ achieves an accuracy of about 10^{-5},and at $h\le1/256, M\ge12$, approximating solution $w_{hM}(x,y)$ achieves an accuracy of about 10^{-4}. In addition, Figure 1-4 also shows that our algorithm is stable and convergent.

Example 2: We consider the case of the radial variable coefficient, taking $\alpha=1, \beta=|\sqrt{(x^2+y^2)}-1/2|, R=1,$ $u=(x^2+y^2-1)^3\cos(xy\pi)e^{\sin(x^2+y^2)}$. Similarly, for different h and M , we list the errors between the exact solution and the approximating solution in Tables 3 and 4. The comparison diagram between the exact solution and the approximating solution is listed in Figure 5 and Figure 6, and the error diagram between the exact solution and the approximating solution is listed in Figure 7 and Figure 8.

International Journal of Scientific Engineering and Science
Volume 8, Issue 12, pp. 59-67, 2024. ISSN (Online): 2456-7361

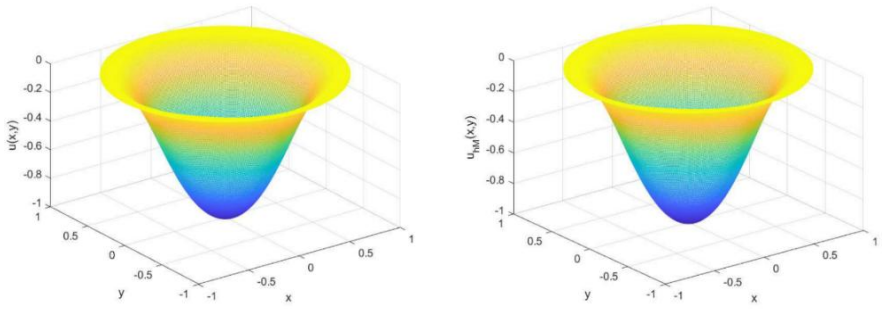

Fig.5 The images of the exact solution u (left) and the approximate solution u_{hM} (right) with $h=1/256, M=12$

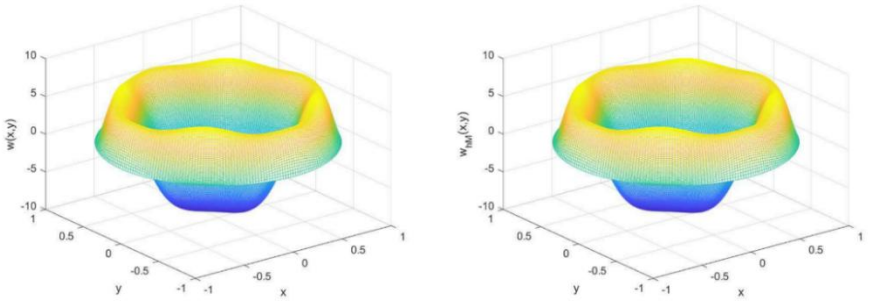

Fig.6 The images of the exact solution w (left) and the approximate solution w_{hM} (right) with $h=1/256, M=12$

Tab.3 The error $e(u,u_{hM})$ between the approximate solution u_{hM} and the exact solution u for different h and M

	$M=4$	$M=8$	$M=12$	$M=16$
$h=1/32$	9.7178295×10^{-3}	1.1492437×10^{-3}	1.1494832×10^{-3}	1.1494833×10^{-3}
$h=1/64$	9.3375552×10^{-3}	2.8657393×10^{-4}	2.8681616×10^{-4}	2.8681615×10^{-4}
$h=1/128$	9.2475774×10^{-3}	7.1436320×10^{-5}	7.1669304×10^{-5}	7.1669303×10^{-5}
$h=1/256$	9.2252993×10^{-3}	1.7687533×10^{-5}	1.7915955×10^{-5}	1.7915954×10^{-5}

Tab.4 The error $e(w,w_{hM})$ between the approximate solution w_{hM} and the exact solution w for different h and M

	$M=4$	$M=8$	$M=12$	$M=16$
$h=1/32$	3.5331859×10^{-1}	1.0710042×10^{-2}	1.1241723×10^{-2}	1.1241077×10^{-2}
$h=1/64$	3.4854456×10^{-1}	3.9740128×10^{-3}	2.8103947×10^{-3}	2.8097327×10^{-3}
$h=1/128$	3.4734356×10^{-1}	3.1927842×10^{-3}	7.0306510×10^{-4}	7.0239922×10^{-4}
$h=1/256$	3.4703430×10^{-1}	3.2345445×10^{-3}	1.7626378×10^{-4}	1.7559694×10^{-4}

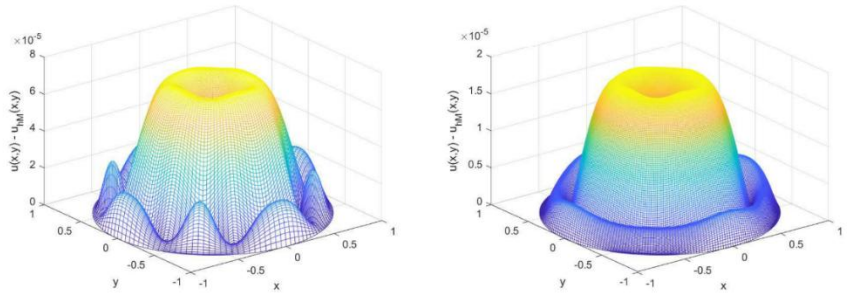

Fig.7 The error images between the exact solution and the approximate solution with $h=1/128, M=8$ (left) and $h=1/256, M=16$ (right)

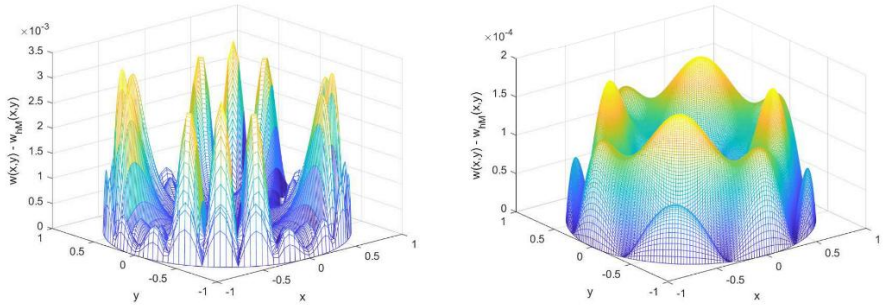

Fig.8 The error images between the exact solution and the approximate solution with $h=1/128, M=8$ (left) and $h=1/256, M=16$ (right)

From Tables 3-4, we observe again that at $h \le 1/128, M \ge 8$, approximating solution $u_{hM}(x,y)$ achieves an accuracy of about 10^{-5}, and at $h \le 1/128, M \ge 12$, approximating solution $w_{hM}(x,y)$ achieves an accuracy of about 10^{-4}. Figure 5-8 shows once again that our algorithm is stable and convergent.

VII. CONCLUSION

In this paper, we propose an efficient hybrid finite element method for solving fourth-order problems in circular domains, which leverages a dimensionality reduction approach. The original problem is reformulated into a sequence of independent, one-dimensional second-order coupled systems. We derive the weak formulation and the corresponding discrete scheme, and rigorously prove the existence and uniqueness of the weak solution, as well as provide theoretical error estimates. The method effectively reduces the high-dimensional problem to a series of one-dimensional problems that can be solved in parallel, yielding significant improvements in computational efficiency and memory usage. Furthermore, the algorithm proposed in this paper can be extended to the computation of fourth-order problems on complex domains, which will be the focus of our future research.

REFERENCES

[1] J. KIM, K. KANG, J. LOWENGRUB. Conservative multigrid methods for Cahn–Hilliard fluids. Journal of Computational Physics, vol. 193, no. 2, pp. 511-543, 2004.
[2] J. GREER, A. BERTOZZI, G. SAPIRO. Fourth order partial differential equations on general geometries. Journal of Computational Physics, vol. 216, no. 1, pp. 216-246, 2006.
[3] X. H. Yang, H. X. Zhang, J. Tang, The OSC solver for the fourth-order sub-diffusion equation with weakly singular solutions, Computers & Mathematics with Applications, vol. 82, pp. 1-12, 2021.
[4] O. LAKKIS, T. PRYER. A finite element method for nonlinear elliptic problems. SIAM Journal on Scientific Computing, vol. 35, no. 4, pp. A2025-A2045, 2013.
[5] B. JIN, R. LAZAROV, Z. ZHOU. Error estimates for a semidiscrete finite element method for fractional order parabolic equations. SIAM Journal on Numerical Analysis, vol. 51, no.1, pp. 445–466, 2013.
[6] J. C. LI. Full-Order Convergence of a Mixed Finite Element Method for Fourth-Order Elliptic Equations. Journal of Mathematical Analysis and Applications, vol. 230, no. 2, pp. 329-349, 1999.
[7] N. PENG, C. WANG, J. AN. An efficient finite-element method and error analysis for the fourth-order elliptic equation in a circular domain. International Journal of Computer Mathematics, vol. 99, no. 9, pp. 1785-1802, 2022.
[8] Y. LI, J. KIM. An efficient and stable compact fourth-order finite difference scheme for the phase field crystal equation. Computer Methods in Applied Mechanics and Engineering, vol. 319, pp. 194-216, 2017.
[9] L. REN, Y. M. WANG. A fourth-order extrapolated compact difference method for time-fractional convection-reaction-diffusion equations with spatially variable coefficients. Applied Mathematics and Computation, vol. 312, pp. 1-22, 2017.
[10] J. AN, J. SHEN. Spectral approximation to a transmission eigenvalue problem and its applications to an inverse problem. Computers & Mathematics with Applications, vol. 69, no.10, pp. 1132-1143, 2015.
[11] T. TAN, W. X. CAO, J. AN. Spectral approximation based on a mixed scheme and its error estimates for transmission eigenvalue problems. Computers & Mathematics with Applications, vol.111, pp. 20-33, 2022.
[12] J.T. JIANG, J. AN, ZHOU J W. A novel numercial method based on a high order polynomial approximation of the fourth order Steklov equation and its eigenvalue problems. Discrete and Continuous Dynamical Systems-Series B, vol. 28, no. 1, pp. 50-69, 2023.